Reconstruction dependent reactivity of As-decapped $In_{0.53}Ga_{0.47}As(001)$ surfaces and its influence on the electrical quality of the interface with Al_2O_3 grown by atomic layer deposition

Cite as: Appl. Phys. Lett. **99**, 193505 (2011); https://doi.org/10.1063/1.3659688
Submitted: 23 December 2010 . Accepted: 19 October 2011 . Published Online: 09 November 2011

A. Molle, L. Lamagna, C. Grazianetti, G. Brammertz, C. Merckling, M. Caymax, S. Spiga, and M. Fanciulli

Reconstruction dependent reactivity of As-decapped $In_{0.53}Ga_{0.47}As(001)$ surfaces and its influence on the electrical quality of the interface with Al_2O_3 grown by atomic layer deposition

A. Molle,[1,a)] L. Lamagna,[1] C. Grazianetti,[1,3] G. Brammertz,[2] C. Merckling,[2] M. Caymax,[2] S. Spiga,[1] and M. Fanciulli[1,3]
[1]*Laboratorio MDM, IMM-CNR, via C. Olivetti 2, I-20864 Agrate Brianza (MB), Italy*
[2]*IMEC, Kapeldreef 75, 3001 Leuven, Belgium*
[3]*Dipartimento di Scienza dei Materiali, Università degli Studi di Milano Bicocca, Milano, Italy*

(Received 23 December 2010; accepted 19 October 2011; published online 9 November 2011)

Tuning the desorption temperature of an As cap layer allows to achieve $In_{0.53}Ga_{0.47}As(001)$ surfaces with (2×4) and (4×2) reconstructions which exhibit different chemical reactivity upon exposure in atmospheric pressure. Trimethyl-Al based atomic layer deposition of Al_2O_3 films on the two exposed surfaces causes a non-equivalent interface composition. This behavior is associated with a worse electrical quality of the interface with the exposed (4×2) $In_{0.53}Ga_{0.47}As$ reconstruction. © *2011 American Institute of Physics*. [doi:10.1063/1.3659688]

In fabricating metal oxide semiconductor (MOS) capacitors on high mobility $In_{0.53}Ga_{0.47}As$ substrates, the electrical activity of interface traps still remains a key issue to assess MOS performances.[1] Intrinsic defect formation occurring in the surface preparation or upon oxide deposition can define the electrical quality of the oxide/semiconductor interface.[2–4] Therefore tuning the chemical bonding at the interface might be crucial for active defects minimization.[5] A close control of the atomic arrangement of $In_{0.53}Ga_{0.47}As(001)$ surfaces can be reached by thermal desorption of an As protective layer[4,6] (As decapping) in ultra high vacuum (UHV) which leads to an (2×4) or a (4×2) reconstruction depending on the decapping temperature T_d.[7] To explore the surface chemistry of both reconstructions and the influence on the electrical interface trapping, this work reports on the trimethyl-Al (TMA)-based atomic layer deposition (ALD) of Al_2O_3 on differently reconstructed $In_{0.53}Ga_{0.47}As(001)$ surfaces after exposure at atmospheric pressure. The $Al_2O_3/In_{0.53}Ga_{0.47}As$ interface composition and the electrical behavior of $Al/Al_2O_3/In_{0.53}Ga_{0.47}As$ MOS capacitors were studied respectively by x-ray photoelectron spectroscopy (XPS) and by admittance analysis.

1 μm-thick n-type (Si doping, $1 \times 10^{17}\,cm^{-3}$) $In_{0.53}Ga_{0.47}As(001)$ samples were grown by molecular beam epitaxy on n-type InP(001) wafers and capped with an As layer which was thermally desorbed in the temperature range 365–440 °C for 15 min in UHV. The As decapping was *in situ* monitored by reflection high energy (30 keV) electron diffraction (RHEED) and the surface structure was then *in situ* scrutinized by scanning tunneling microscopy (STM). The so-prepared surfaces were moved in atmospheric pressure (3 min in N_2 flow) to a Savannah ALD reactor (Cambridge Nanotech) where Al_2O_3 films were grown at 300°C as follows: 500 ms TMA pulse, 8 s N_2 purge, 15 ms H_2O pulses, and 8 s N_2 purge. Thin films (2 nm) were grown for XPS investigation of the $Al_2O_3/In_{0.53}Ga_{0.47}As$ interface via standard Mg and Al Kα radiation sources with a pass energy of 20 eV and a take-off angle of 70°. MOS capacitors were then fabricated by thermally evaporating 100 nm Al dot electrodes (diameter of 150 μm) on 13 nm-thick Al_2O_3 with no post-deposition annealing. Multifrequency ($f = 100$ Hz–1 MHz) capacitance-voltage (C-V_g) and conductance-voltage (G-V_g) characteristics (corrected for series resistance) were recorded with temperature varying from 77 to 300 K in dark through an Agilent HP4284A LCR meter.

Two different $In_{0.53}Ga_{0.47}As$ surface reconstructions are evidenced in Fig. 1 by RHEED patterns with beam directions along the two orthogonal azimuths, [110] and [−110], after decapping at $T_d = 365$°C (Fig. 1(a)) and 440°C (Fig. 1(b)), respectively named as low-T and high-T sample in the following. Upon low-T decapping, from Fig. 1(a) 2× and 4× periodicities result along the [−110] and [110] axes which correspond to an As-rich (2×4) reconstruction.[7] When

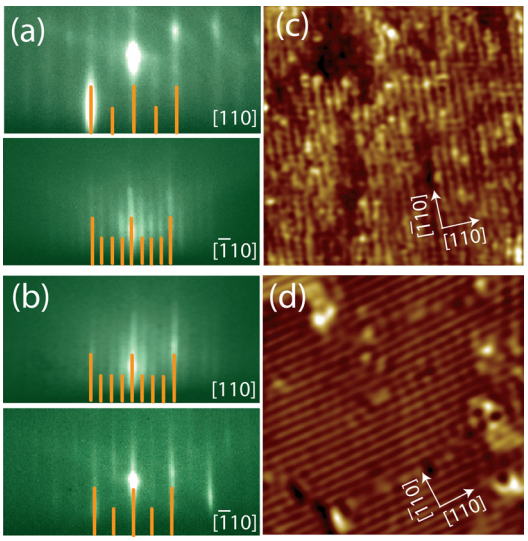

FIG. 1. (Color online) RHEED pattern after As decapping at 365°C (a) and at 440 °C (b) for a beam direction along the azimuths [110] (top image) and [−110] (bottom image). The beam direction is reported in each pattern. (c),(d) $50 \times 50\,nm^2$ STM topographies measured after As decapping at 365°C and 440°C (low-T and high-T surface, respectively). Imaging conditions are constant-current mode with a typical 0.5–2 nA setpoint tunneling current and −1.5 V sample bias voltage (filled states images). Arrows in panel (d) mark the surface azimuths.

a)Electronic mail: alessandro.molle@mdm.imm.cnr.it.

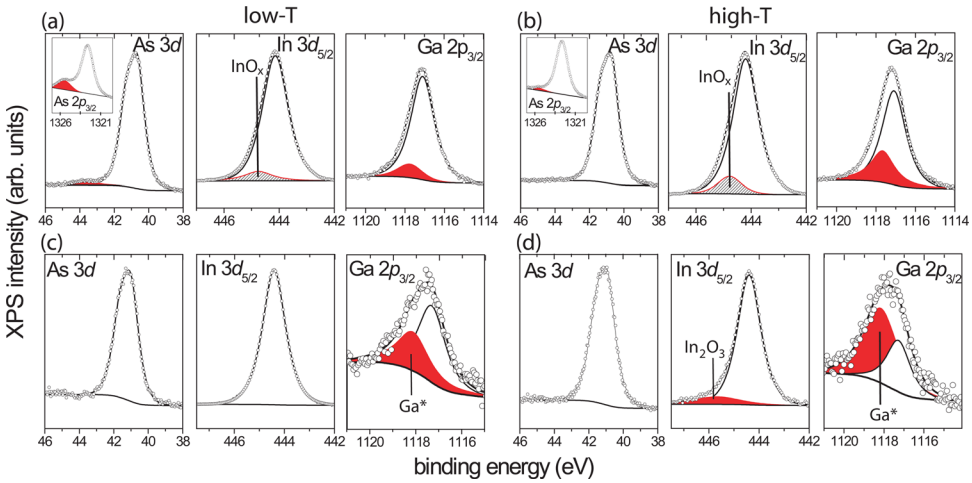

FIG. 2. (Color online) XPS As 3*d*, In $3d_{5/2}$, Ga $2p_{3/2}$ lines taken upon exposure on the low-T surface (a) and high-T surface (b) (insets show the related As $2p_{3/2}$ lines); XPS As 3*d*, In $3d_{5/2}$, Ga $2p_{3/2}$ lines taken after subsequent ALD of a 2 nm-thick Al_2O_3 film on the exposed low-T (c) and high-T surfaces (d).

annealed at 440°C the previous configuration is switched in a group III-rich (4×2) reconstruction with $4\times$ and $2\times$ periodicities along the [−110] and [110] axes, respectively (Fig. 1(b)). This scenario is confirmed by the $50 \times 50\,nm^2$ STM topographies in Figs. 1(c) and 1(d), which respectively visualize a (2×4) and a (4×2) reconstruction. The (2×4) reconstruction consists of As dimer rows along the [−110] axis divided by trough regions [Fig. 1(c)]. The (4×2) reconstruction shows more ordered rows along the [110] axis [Fig. 1(d)] with a mean separation of 1.7 nm.

The chemical reactivity of the two surfaces is studied by probing the As 3*d*, In $3d_{5/2}$, and Ga $2p_{3/2}$ XPS lines after exposure (see Figs. 2(a) and 2(b) for the low-T and high-T surface, respectively). The spectra were decomposed with pseudo Voigt functions (doublets for the As 3*d* line) upon Shirley background removal. Fit to the spectra was based on the shape profile of bulk peaks in the pristine reconstructed surfaces.[8] Limited adventitious carbon contamination has been observed after exposure. The As 3*d* line of the high-T surface is rid of As oxides whereas a As_2O_3 can be deduced from the low-T surface. To gain a higher surface sensitivity, the As $2p_{3/2}$ lines are reported in the insets of Figs. 2(a) and 2(b) which evidence the formation of As_2O_3 on the low-T surface and minor trace of As_2O_3 also in the high-T surface upon exposure. The In $3d_{5/2}$ and Ga $2p_{3/2}$ lines exhibit an extra-component indicative of chemisorbed species along with the bulk one. In both In $3d_{5/2}$ lines the extra-component can be associated with sub-stoichiomteric InO_x because the chemical shift Δ is lower than that reported for the In_2O_3 (Refs. 9 and 10), whereas $\Delta = 0.6\,eV$ in the Ga $2p_{3/2}$ lines is consistent with Ga_2O species.[3,11] A larger amount of In-O and Ga-O bonds is revealed after exposure of the high-T surface. The effect of the ALD cycles on the interface chemistry is elucidated by the As 3*d*, In $3d_{5/2}$, and Ga $2p_{3/2}$ XPS lines in Figs. 2(c) and 2(d) recorded after deposition of 2 nm-thick Al_2O_3 film on the two surfaces. Within the XPS detection limits, the As 3*d* lines evidence an As oxide-free surface on both samples. From the In $3d_{5/2}$ lines, InO_x disappears in the low-T sample whereas formation of In_2O_3 is observed in the high-T sample which indicates further In oxidation. The Ga $2p_{3/2}$ lines can be decomposed in a bulk peak and a Ga* component with $\Delta = 0.9\,eV$ consistent with the interplay of interfacial Ga_2O_3 and Ga_2O.[3] Important is to note that: (a) Ga–O bonds increases after ALD cycles despite the previously reported reducing effect played by TMA on both As and Ga oxides in a different extent (the so-called TMA "self-cleaning")[10,12,13]; (b) the relative intensity of Ga*, i.e., the amount of Ga oxides, is much higher in the high-T sample than in the low-T one.

From the electrical viewpoint, C-V_g characteristics of the MOS capacitors based on the low-T and high-T samples were recorded at 300 K (Figs. 3(a) and 3(b)) and at 150 K (Figs. 3(c) and 3(d)) The C-V_g curves at 300 K of both capacitors exhibit a similar high frequency inversion behavior which can originate either from the electrical activity of midgap interface traps[6] or from the minority carrier response.[12] The C-V_g characteristics taken at 150 K are also reported in Figs. 3(c) and 3(d) for both samples where the depletion behavior is dictated by interface traps.[14] From Figs. 3(c) and 3(d) a more pronounced stretch-out of the C-V_g curves takes place in the high-T sample which is related to a higher density of interface traps (D_{it}).[3–5,7] The insets of Figs. 3(c) and 3(d) show a similar hysteresis behavior of the two MOS capacitors at 150 K and 1 MHz which indicate similar amounts of charging defects in the oxide. The accumulation capacitance (C_{acc}) of the C-V_g curves is plotted as a function of f in Figs. 4(a) and 4(b) respectively for the low-T and high-T MOS capacitors for various temperatures. Both diagrams evidence a temperature dependent dispersion of C_{acc} over four frequency decades.

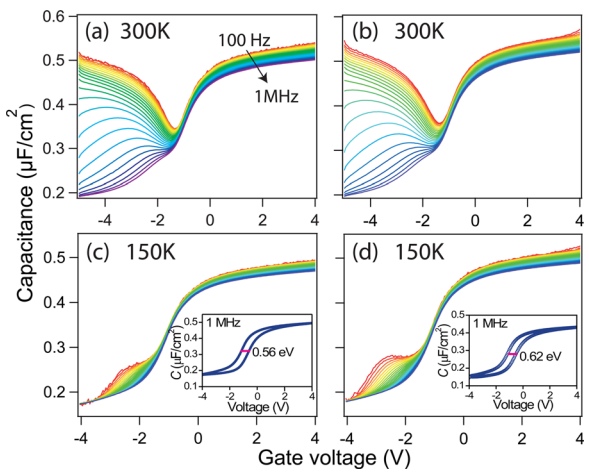

FIG. 3. (Color online) Multifrequency C-V_g characteristics of MOS capacitors: 300 K (a) and 150 K (c) for the low-T sample; 300 K (b) and 150 K (d) for the high-T sample. Insets: 1 MHz C-V_g curves with hysteresis taken at 150 K for the low-T (left) and for the high-T sample (right).

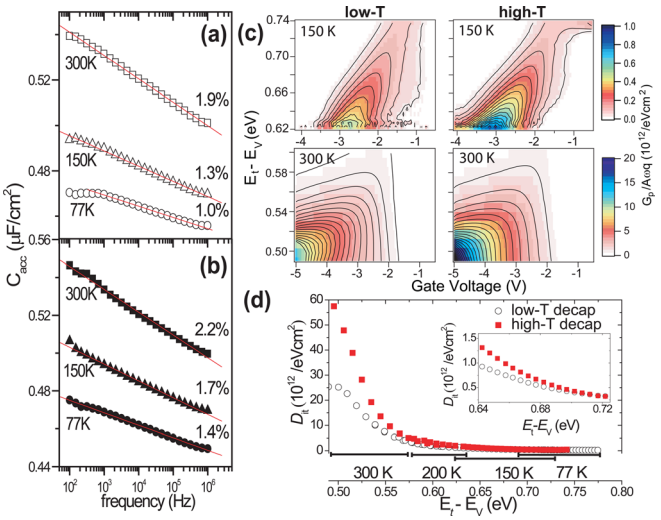

FIG. 4. (Color online) Plot of the capacitance in accumulation (C_{acc}) vs frequency at 300, 150, and 77 K for the low-T (a) and high-T samples (b) (accumulation dispersion per decade is reported for each plot). (c) Conductance maps recorded at 150 K (upper) and 300 K (downer) in MOS capacitors based on the low-T (left) and high-T sample (right). (d) D_{it} vs E_t diagram in the energy range $0.48\,\text{eV} < E_t < 0.80\,\text{eV}$ (measured from the valence band maximum). Inset: magnification of the D_{it} diagram for $0.64\,\text{eV} < E_t < 0.72\,\text{eV}$.

Slopes extracted for the high-T sample are larger than those of the low-T one (2.2%, 1.7%, and 1.4% vs 1.9%, 1.3%, 1.0% per decade respectively for 300, 150, and 77 K). The temperature dependent frequency dispersion of C_{acc} in both cases can be related to thermally activated trapping through interface states.[6] Though not resolvable, an additional contribution to this behavior might also come from border traps in Al_2O_3.[15] The substrate conductance $G_p/A\omega q$ (G_p is the conductance corrected for the oxide capacitance,[14] A the dot area, q the electron charge, and $\omega = 2\pi f$ the pulsation) is examined at 77, 150, 200, and 300 K in order to plot the D_{it} vs the trap energy levels (E_t) in the upper half side of the bandgap. Conductance maps recorded at 300 and 150 K are plotted in Fig. 4(c) for the two MOS capacitors as a function of V_g (x axis) and of E_t (y axis) computed by assuming a capture cross section $9.2 \times 10^{-17}\,\text{cm}^2$.[6] The $G_p/A\omega q$ peak trace in the maps shows that the interface Fermi level can be freely moved under gate control and identify different D_{it} distributions between the two MOS capacitors.[10] Significantly low $G_p/A\omega q$ peak traces are measured in the map at 150 K near the conduction band (CB) edge for both samples ($0.68\,\text{eV} < E_t < 0.74\,\text{eV}$) whereas a more intense $G_p/A\omega q$ peak trace is observed in the map of the high-T sample for $E_t < 0.68\,\text{eV}$ therein indicating a higher D_{it}. A remarkable deviation between the samples can be observed at 300 K, as the high-T sample exhibit higher $G_p/A\omega q$ peaks than the low-T sample. In Fig. 4(d) the D_{it} is evaluated for the two MOS capacitors as a function of E_t from Gaussian fits to the $G_p/A\omega q$ peaks extracted at 77, 150, 200, and 300 K in order to probe different energy regions.[14] Little D_{it} difference occurs near the CB edge, where D_{it} is limited to the low-$10^{11}\,\text{eV}^{-1}\,\text{cm}^{-2}$ range. A larger deviation appears with decreasing E_t from 0.68 to 0.53 eV (inset of Fig. 4(d)). The D_{it} severely increases towards midgap in agreement with previous reports,[6,7,9] but with a different extent in the two samples, i.e., remarkably higher in the high-T sample.

The different D_{it} fashions in the two samples can be attributed to the observed reconstruction-dependent surface chemistry against exposure which affects the interface composition with the subsequently grown Al_2O_3 (see Fig. 2). Despite the As-rich (2×4) reconstruction in the low-T sample undergoes an easier oxidation of As dimers[4] thus rendering the exposed (2×4) surface richer of As_2O_3 (see Fig. 2(a)), XPS data in Figs. 2(c) and 2(d) show surface As–O bonds to be more efficiently reduced by the initial TMA pulse with respect to the Ga–O and In–O ones in both samples.[16] As a consequence, a significantly higher content of interfacial Ga–O (interplay of Ga_2O and Ga_2O_3) and In–O (In_2O_3) bonds results in the interface between Al_2O_3 and the exposed (4×2) reconstructed $In_{0.53}Ga_{0.47}As(001)$ surface (high-T sample) because Ga–O and In–O bonds can more readily form upon oxygen chemisorption to Ga an In onto the rows along the [110] direction (see Fig. 1(b)) as observed on InAs(001).[17] The higher midgap D_{it} and the worse electrical response of the C-V_g curves (i.e., larger stretch-out and dispersion in accumulation) measured on the MOS capacitors based on the high-T sample can be then ascribed to the larger amounts of Ga–O and In–O interfacial bonds. The peculiar surface reactivity and interaction with the initial TMA pulse makes the low-T decapping, i.e., the (2×4) $In_{0.53}Ga_{0.47}As(001)$ reconstruction, more prone to limit interfacial Ga–O and In–O bonds therein reducing electrically active interface traps.

We acknowledge grant from ARAMIS Project and M. Alia (MDM) for metal gate deposition.

[1]D. Peide and J. Ye, Vac. Sci. Technol. A **26**(4), 697 (2008).
[2]J. Robertson, Appl. Phys. Lett. **94**, 152104 (2009).
[3]C. L. Hinkle, M. Milojevic, B. Brennan, A. M. Sonnet, F. S. Aguirre-Tostado, G. J. Hughes, E. M. Vogel, and R. M. Wallace, Appl. Phys. Lett. **94**, 162101 (2009).
[4]B. Shin, J. Clemens, M. A. Kelly, A. C. Kummel, and P. C. McIntyre, Appl. Phys. Lett. **96**, 252907 (2010).
[5]Y. C. Chang, C. Merckling, J. Penaud, C. Y. Lu, W.-E. Wang, J. Dekoster, M. Meuris, M. Caymax, M. Heyns, J. Kwo, and M. Hong, Appl. Phys. Lett. **97**, 112901 (2010).
[6]Y. Hwang, M. A. Wistey, J. Cagnon, R. Engel-Herbert, and S. Stemmer, Appl. Phys. Lett. **94**, 122907 (2009).
[7]J. Shen, D. Winn, W. Melitz, J. Clemens, and A. C. Kummel, ECS Trans. **16**, 463 (2008).
[8]L. Lamagna, M. Fusi, S. Spiga, M. Fanciulli, G. Brammertz, C. Merckling, M. Meuris, and A. Molle, Microelectr. Eng. **88**, 431 (2011).
[9]A. P. Kirk, M. Milojevic, J. Kim, and R. M. Wallace, Appl. Phys. Lett. **96**, 202905 (2010).
[10]H. D. Trinh, E. Y. Chang, P. W. Wu, Y. Y. Wong, C. T. Chang, Y. F. Hsieh, C. C. Yu, H. Q. Nguyen, Y. C. Lin, K. L. Lin, and M. K. Hudait, Appl. Phys. Lett. **97**, 042903 (2010).
[11]A. Molle, G. Brammertz, L. Lamagna, M. Fanciulli, M. Meuris, and S. Spiga, Appl. Phys. Lett. **95**, 023507 (2009).
[12]H.-C. Lin, W.-E. Wang, G. Brammertz, M. Meuris, and M. Heyns, Microelectr. Eng. **86**, 1554 (2009).
[13]A. O'Mahony, S. Monaghan, G. Provenzano, I. M. Povey, M. G. Nolan, É. O'Connor, K. Cherkaoui, S. B. Newcomb, F. Crupi, P. K. Hurley, and M. E. Pemble, Appl. Phys. Lett. **97**, 052904 (2010).
[14]E. H. Nicollian and J. R. Brews, *MOS (Metal Oxide Semiconductor) Physics and Technology* (Wiley, New York, 1982).
[15]E. J. Kim, L. Wang, P. M. Asbeck, K. C. Saraswat, and P. C. McIntyre, Appl. Phys. Lett. **96**, 012906 (2010).
[16]M. Milojevic, F. S. Aguirre-Tostado, C. L. Hinkle, H. C. Kim, E. M. Vogel, J. Kim, and R. Wallace, Appl. Phys. Lett. **93**, 202902 (2008).
[17]J. B. Clemens, S. R. Bishop, D. L. Feldwinn, R. Droopad, and A. C. Kummel, Surf. Sci. **603**, 2230 (2009).